Spin Conversion Processes in Solutions

E. Buhks, G. Navon,* M. Bixon,* and J. Jortner*

Contribution from the Department of Chemistry, Tel-Aviv University, Tel Aviv, Israel. *Received August 6, 1979*

Abstract: High-spin to low-spin crossover processes in some transition-metal complexes are described in terms of a radiationless nonadiabatic multiphonon process, occurring between two distinct zero-order spin states, which are characterized by different nuclear configurations. The rate constant was expressed in terms of separate electronic and nuclear contributions. An evaluation of the electronic spin-orbit coupling terms is reported, while the nuclear vibrational overlap factors were estimated from spectroscopic and structural data. The calculated rate constants for spin crossover in some Fe(II) and Fe(III) complexes are calculated without introducing any adjustable parameters and are in order-of-magnitude agreement with the available experimental data.

I. Introduction

It is one of the predictions of the ligand field theory that octahedral complexes of d^4–d^7 transition metal ions may occur in high- or low-spin forms depending on whether the ligand-field splitting is smaller or greater than the interelectronic repulsion energies. Early measurements of magnetic susceptibilities of tris(dithiocarbamato)iron(III)[1] complexes indicated that, depending on their substituents, these complexes can be in high spin, low spin, or spin equilibrium. Since this observation was reported more systems were found to be in spin equilibrium.[2,3] Recently, rates of spin crossover were measured for a number of systems in solution containing iron(II),[4-8] iron(III),[7,9-12] and cobalt(II)[13] using the Raman laser temperature-jump and ultrasonic absorption techniques. The measured unimolecular rates for all systems investigated up to date are in the range of 10^6–10^9 s^{-1}. An attempt to provide a theoretical description of such spin conversion processes was provided by Dose and colleagues,[7] who started from absolute reaction rate theory, estimating the transmission coefficient from the semiclassical Landau–Zener formula and providing a classical description of the activation energy in terms of inner-sphere reorganization energy. In this paper we advance a general theoretical framework for the description of such processes. We propose that the spin crossover process can be described in terms of a radiationless multiphonon process occurring between two distinct (zero order) spin states, which are characterized by different nuclear equilibrium configurations.[14-16] We shall present an attempt to calculate spin conversion rates in terms of such theory. Although the results of the calculations are in good agreement with the available experimental data, they should be considered only as a first approximation and may be helpful in order to assess the various factors that determine the spin conversion rates.

Our analysis is restricted to the situation where the two spin states are characterized by different nuclear configurations, being separated by an energy barrier which is large relative to the thermal energy k_BT. In the transition-metal complexes this configurational difference is manifested in terms of a stretched metal–ligand bond in the high-spin state, as compared to the low-spin state. Other interesting situations, corresponding to spin crossover processes in condensed phases involving the recombination of O_2 or CO with hemoglobin or myoglobin,[14] can also be described in terms of radiationless multiphoton processes.[14b] However, the nature of the nuclear configurational changes is more complex in the latter case than for spin conversion in transition-metal complexes.

II. Theory

The spin conversion processes we are considering here are radiationless transitions between two electronic states of the same complex, having two different spin states and slightly different nuclear equilibrium configurations. The general theory of multiphonon radiationless transitions, in a form similar to its application to the theory of electron-transfer reactions in solution, may be applied.[15-17]

The intramolecular spin conversion in solution is described as a transition between an initial manifold of states $\psi_i(\vec{r},q_c)\chi_{\kappa_i}(q_c)\phi_{n_i}(q_s)$ with energies $E_i + E^c_{\kappa_i} + E^s_{n_i}$ and a final manifold of states $\psi_f(\vec{r},q_c)\chi_{\kappa_f}(q_c - \Delta_c)\phi_{n_f}(q_s - \Delta_s)$ with energies $E_f + E^c_{\kappa_f} + E^s_{n_f}$, where the indexes c and s stand for the internal modes and the solvent modes, respectively. ψ_i and ψ_f represent the electronic wave functions in the initial and final states, respectively, while E_i and E_f are the electronic energies in the initial and in the final states, respectively. $(E^c_{\kappa_i} + E^s_{n_i})$ and $(E^c_{\kappa_f} + E^s_{n_f})$ denote the energies of the vibrational levels in both states, each corresponding to separate contributions, i.e., E^c from the internal modes and E^s from the solvent. The electronic coordinates are $\vec{r}$, while nuclear coordinates are represented by q_c and q_s. χ_κ and ϕ_n are the harmonic oscillator nuclear states of the internal modes and of the solvent. Owing to configurational changes and different interactions with the solvent in the initial and final states, the oscillators describing the harmonic nuclear potential surfaces are displaced in the final state by the quantities Δ_c and Δ_s relative to the initial state. The product wave functions $\psi(\vec{r},q_c)\chi_{\kappa_i}(q_c)$ and $\psi_f(\vec{r},q_c)\chi_{\kappa f}(q_c - \Delta_c)$ are the pure spin molecular Born–Oppenheimer states.

Owing to the existence of spin–orbit interaction, H_{so}, the correct initial and final states are not exactly pure spin states. The admixture with higher electronic states $\{\psi_m\}$ may be ignored if there exists a direct coupling between the initial and final pure spin states; otherwise one has to use a better representation for the electronic wave functions. To first order in perturbation theory one gets for the initial state

$$\psi_i' = \psi_i + \sum_m \frac{\langle \psi_i | H_{so} | \psi_m \rangle}{(E_i - E_m)_{q_i}} \psi_m \qquad (1)$$

where the energy difference $(E_i - E_m)$ is evaluated at the minimum energy configuration of the initial state. A similar expression may be written down for the final state, in which case the denominator has to be evaluated at the configuration of the final state.

Disregarding external perturbations, the coupling between the initial and final states is caused by the spin–orbit interaction operator. Assuming that the spin conversion is a nonadiabatic process, one can write the following formal Golden rule expression for the rate constant:[15,16]

$$k = \frac{2\pi}{\hbar} g_f A v_{\kappa_i n_i} \sum_{\kappa_f n_f} \delta(\Delta E + E^c_{\kappa_f} + E^s_{n_f} - E^c_{\kappa_i} - E^s_{n_i}) \otimes |\langle \psi_i' | H_{so} | \psi_f' \rangle \langle \chi_{\kappa_i} | \chi_{\kappa_f} \rangle \langle \phi_{h_i} | \phi_{n_f} \rangle|^2 \qquad (2)$$

0002-7863/80/1502-2918$01.00/0

where g_f is the degeneracy of the final electronic state and $Av_{\kappa_i n_i}$ stands for the operation of thermal averaging over the initial vibrational states:

$$Av_{\kappa_i n_i}(\bullet) = (Z^s{}_i Z^c{}_i)^{-1} \sum_{\kappa_i n_i} \exp[-(E^s{}_{n_i} + E^c{}_{\kappa_i})/k_B T]\,(\bullet) \quad (2a)$$

Here, $Z^s{}_i = \Sigma_{n_i} \exp(-E^s{}_{n_i}/k_B T)$ and $Z^c{}_i = \Sigma_{\kappa_i} \exp(-E^c{}_{\kappa_i}/k_B T)$ are the partition functions for the nuclear motion of the solvent and of the internal motion of the complex, respectively. ΔE is the electronic energy gap $\Delta E = E_f - E_i$. Equation 2 constitutes a general nonadiabatic multiphonon rate constant. The nonadiabatic approximation applies only if the perturbation matrix elements are sufficiently small. We would like to emphasize that the quantity one has to check for smallness is not just the electronic matrix element but rather the molecular vibronic matrix element. We shall return to this point in section V.

The expression for the rate constant may be conveniently written as

$$k = (2\pi/\hbar) g_f |V|^2 G \quad (3)$$

where V represents the electronic coupling matrix element

$$V = \langle \psi_i' | H_{so} | \psi_f' \rangle = \langle \psi_i | H_{so} | \psi_f \rangle + \sum_m \langle \psi_i | H_{so} | \psi_m \rangle \langle \psi_m | H_{so} | \psi_f \rangle \times [(E_i - E_m)^{-1} q_i + (E_f - E_m)^{-1} q_f] \quad (4)$$

The contribution of the solvent modes and of the inner vibrations is given by the thermally averaged nuclear Franck-Condon vibrational overlap factor G defined as

$$G = (Z^s{}_i Z^c{}_i)^{-1} \sum_{\kappa_i n_i \kappa_f n_f} \exp[-(E^s{}_{n_i} + E^c{}_{\kappa_i})/k_B T] \times |(\chi_{\kappa_i} | \chi_{\kappa_f})\,(\phi_{n_i} | \phi_{n_f})|^2\, \delta(\Delta E + E^s{}_{n_f} + E^c{}_{\kappa_f} - E^s{}_{n_i} - E_{\kappa_i}) \quad (5)$$

In order to get an analytic expression for G we have to use a sufficiently simple model for the vibrational modes of the system. Our model is based on the very reasonable assumption that the solvent may be represented by very low frequency oscillators (so that $\hbar\omega_s \ll k_B T$) and, therefore, the solvent contribution to the rate constant can be expressed in terms of a single parameter, E_s, the solvent reorganization energy. To simplify matters further, we neglect frequency changes between the initial and the final states and assume that only one internal mode with frequency ω, and with the displacement Δr, contributes to G. In this case one gets the expression[16]

$$G(\Delta E, \omega, S, E_s, T) = \frac{1}{\hbar\omega}\left(\frac{x}{2\pi q}\right)^{1/2} \sum_{m=-\infty}^{\infty} I_m\left(\frac{S}{\sinh x}\right) \times \exp[-S \coth x - mx - (p + q - m)^2 x/2q] \quad (6)$$

where $x = \hbar\omega/2k_B T$ is the reduced internal frequency, $q = E_s/\hbar\omega$ is the reduced solvent reorganization energy, $p = \Delta E/\hbar\omega$ is the reduced electronic energy gap, and $I_m(\bullet)$ is the modified Bessel function of order m. The coupling parameter S measures the contribution of the change in the internal normal mode

$$S = m\omega(\Delta r)^2/2\hbar \quad (7)$$

Unlike the case of electron-transfer reactions, where the repolarization energy, originating from long-range Coulombic interactions, is large,[16] the solvent reorganization energy in the spin conversion case, which results from short-range complex solvent interactions, is quite small. In principle, it cannot be ignored because the solvent provides the continuum of states required for the transition. But, in practice, when its value is in the range of tens to hundreds cm^{-1}, the contribution from the continuous phonon spectrum of the medium modes provides a sufficient broadening mechanism at room temperature. Consequently, we may use the one-mode expression[16] for the thermally averaged nuclear vibrational overlap factor

$$G = \frac{1}{\hbar\omega} \exp[-S \coth x - px]\, I_p\left(\frac{S}{\sinh x}\right) \quad (8)$$

This expression is meaningful only for discrete values of p, but the broadening provided by E_s permits us to interpolate between them. When E_s is small enough ($\sim$50–100 cm^{-1}), as we expect to be the case here, one gets almost the same numerical values for G from eq 6 and 8. This is evident from the results of Figure 1, which displays G calculated from eq 8 and 6 for $q = 0.3$.

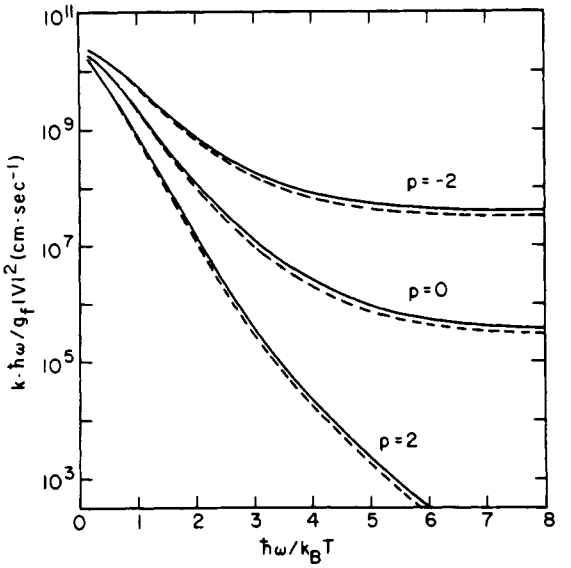

Figure 1. A comparison between the temperature dependence of the spin-conversion rate constant as calculated from the single-mode approximation, eq 8, (solid lines), and from eq 6 with the solvent reorganization parameter $q = 0.3$ (dashed lines). Data given for $p = -2$, 0, and +2 in the strong coupling limit $S = 15$.

Equation 8 may provide approximate results for systems with more than a single displaced mode, if we interpret ω as an average over the vibrational frequencies and take S to be the sum of their contributions. A graphical representation of the rate constant for a reasonable range of parameters is given in Figure 2. Taking the temperature derivatives of eq 8, one obtains the activation energy, which is portrayed in Figure 3. Figures 1–3 reveal that the conventional Arrhenius form of the rate constant is limited to the high-temperature range. For exoergic and isoenergetic processes ($\Delta E \leq 0$) the rate constant flattens off at low temperatures ($k_B T \ll \hbar\omega$), whereupon the activation energy vanishes. The finite low-temperature rate constant reflects the occurrence of nuclear tunnelling.[14b,15,16] For endoergic processes ($\Delta E > 0$) the reaction is activated also at low temperatures. The low-temperature activation energy is $E_A(T \to 0) = \Delta E$; as now, to ensure energy conservation, nuclear tunnelling can prevail only at the energy ΔE above the origin of the initial potential surface.

One shortcoming of the theory is its incomplete consideration of the reaction entropy. Spin multiplicities are fully taken into account but entropy changes due to solvent orientation are ignored. This causes some ambiguity in the proper choice of the thermodynamic parameter p. As the free energy of reaction for all the systems whose spin conversion rates were measured is approximately zero, we decided to base our analysis of these systems on the value $p = 0$. Undoubtedly, this choice may introduce some uncertainty in the computed rates. Our analysis is based on the use of Figure 4, in which the rate constant is

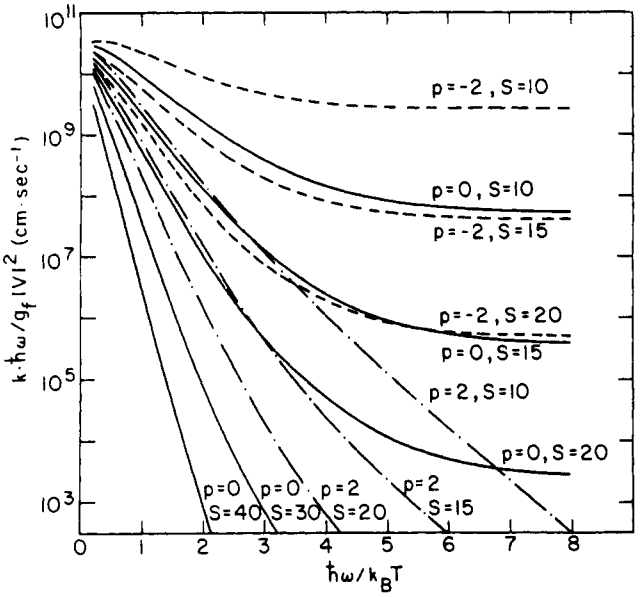

Figure 2. Model calculations in the single-mode approximation for the nuclear contribution to the rate constant of spin-conversion processes. $p = -2$, 0, and +2; S = 10–40.

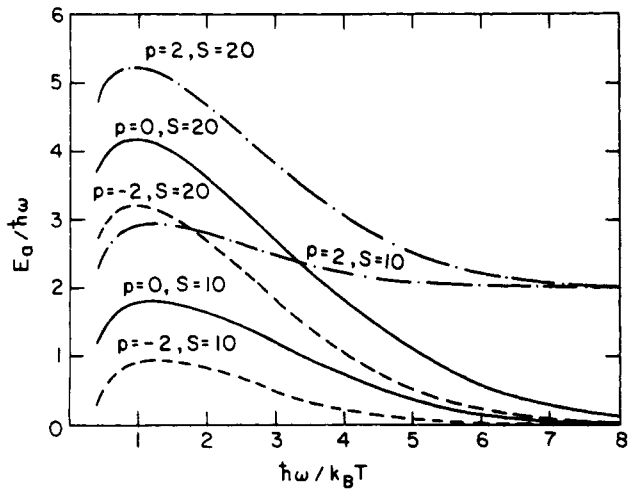

Figure 3. The temperature dependence of the activation energy of the spin-conversion process.

given as a function of S for different values of $\hbar\omega/k_BT$, and where everything is computed for the specific case $p = 0$.

The spin conversion rate constant, eq 3, is expressed in terms of a product of an electronic spin–orbit matrix element V and a nuclear Franck–Condon factor G, separating electronic and nuclear contributions to the dynamics of the process. We now proceed to consider separately these two ingredients.

III. Calculation of Electronic Matrix Elements

In the present calculations we assume, for the sake of simplicity, that the complex is characterized by octahedral symmetry. The perturbation H_{so} being a one-electron operator, we can distinguish between two types of spin conversion processes: (a) Only the one electron state is changed upon the transition and, therefore, the first term in eq 4 is different from zero. This happens when the electronic configuration is d^4 or d^7. (b) Two electrons are involved in the transition. In this case, the first term in eq 4 vanishes and one has to use the second term. This is also the case for the electronic configuration d^5 or d^6.

d^6 Ions (Fe(II), Co(III)). The electronic configurations t_{2g}^6 and $t_{2g}^4e_g^2$ of the low-spin and the high-spin forms correspond to ^1A_g and to $^5T_{2g}$ ground-state terms, respectively. Spin–orbit coupling interactions have vanishing matrix elements between these two terms. The only term which has nonvanishing matrix elements with both ^1A_g and $^5T_{2g}$ is the $^3T_{1g}$ term of the intermediate electronic configuration $t_{2g}^5e_g$:[18]

$$\langle {}^1A_{1g} | H_{so} | {}^3T_{1g} \rangle = -\sqrt{6}\zeta \qquad (9)$$
$$\langle {}^5T_{2g} | H_{so} | {}^3T_{1g} \rangle = \sqrt{3}\zeta$$

where ζ is the spin–orbit coupling constant. Thus according to eq 4

$$V = -3\sqrt{2}\zeta^2 \left(\frac{1}{\Delta E_1} + \frac{1}{\Delta E_2} \right) \qquad (10)$$

where ΔE_1 is the energy difference between the $^3T_{1g}$ state and $^1A_{1g}$ at the equilibrium configuration of $^1A_{1g}$ and ΔE_2 is the energy difference between $^3T_{1g}$ and $^5T_{2g}$ at the equilibrium configuration of $^5T_{2g}$. In the present case these energy differences are approximately equal, within the uncertainties in their values. An approximation of this energy gap can be obtained from the energy-level diagrams of Tanabe and Sugano.[19] The diagram for d^6, which was calculated under the assumption $C/B = 4.81$, gives at the crossing point $\Delta E = 7.6B$. The values of B and C are different for each complex, according to the nephelauxetic effect,[20] being smaller than the free ion values. However, it is interesting to note that also the spin–orbit coupling constant ζ is reduced by covalency relative to its free ion value. Therefore, the covalency effects on B and C and on ζ are expected to cancel each other in the second-order perturbation term of eq 4 and 10. The reason for it can be seen from the structure of the molecular orbitals, as described in the equation

$$\psi = a\psi_{metal} - b\psi_{ligand} \qquad (11)$$

The constants B and C are expected to be proportional to a^4, while ζ is proportional to a^2.[21]

From the free ion values of B = 1058 cm^{-1} [18] and ζ = 400 cm^{-1} [22] for Fe(II) and B = 1065 cm^{-1} [19] and ζ = 580 cm^{-1} [22] for Co(III), we estimate $|V|$ = 170 cm^{-1} for Fe(II) and $|V|$ = 380 cm^{-1} for Co(III).

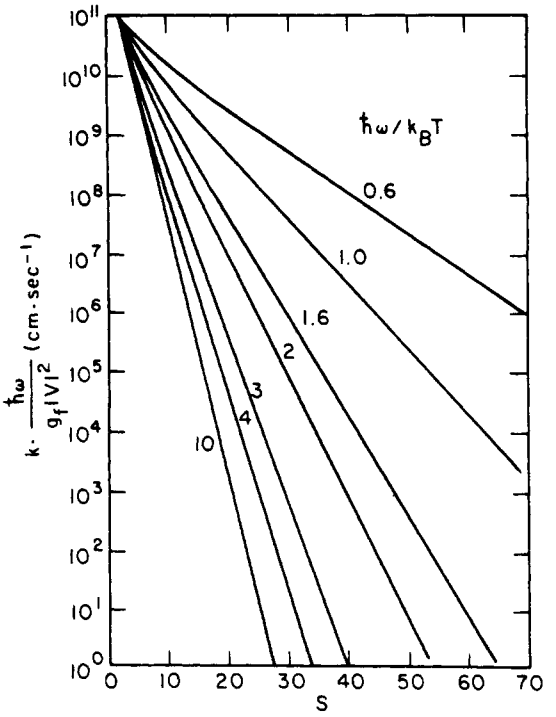

Figure 4. The rate constant of the isoenergetic spin-conversion process vs. the coupling strength parameter, S. Data given for various temperatures.

d^5 Ions (Fe (III), Mn(II)). The calculations in this case follow closely those of the d^6 case. The low-spin t_{2g}^5 ground state is $^2T_{2g}$ and that of the high-spin $t_{2g}^3e_g^2$ is $^6A_{1g}$. The only terms which have nonvanishing matrix elements with both $^2T_{2g}$ and $^6A_{1g}$ are the components $^4T_{1g}(E'')$ and $^4T_{1g\ 5/2}(U')$ of the spin-orbit multiplet of the term $^4T_{1g}(t_{2g}^4e_g)$.[18]

$$\begin{aligned}\langle {}^6A_{1g}|H_{so}|{}^4T_{1g}(E'')\rangle &= -\sqrt{2}\zeta\\ \langle {}^2T_{2g}|H_{so}|{}^4T_{1g}(E'')\rangle &= \sqrt{3}\zeta\\ \langle {}^6A_{1g}|H_{so}|{}^4T_{1g5/2}(U')\rangle &= -\sqrt{2}\zeta\\ \langle {}^2T_{2g}|H_{so}|{}^4T_{1g5/2}(U')\rangle &= -\sqrt{6/5}\zeta\end{aligned} \tag{12}$$

Thus, neglecting the energy difference within the spin-orbit multiplet relative to the energy difference with other terms, we obtain (using eq 4)

$$V = 1.8\zeta^2/\Delta E \tag{13}$$

An estimate for the value of the average energy difference ΔE is obtained from the Tanabe and Sugano diagrams (with $C/B = 4.48$),[23] as $\Delta E = 8.4B$. Using the free ion values for Fe(III) $B = 1015$ cm^{-1} [19] and $\zeta = 460$ cm^{-1},[22] we obtain $V = 44$ cm^{-1}.

d^4 Ions (Cr(II), Mn(III)). The ground-state term of the low-spin t_{2g}^4 electronic configuration, $^3T_{1g}$, in octahedral fields is split by the spin-orbit interaction to the terms (in the double-group scheme) A_1, T_1, E_2, and T_2 with energies $-\zeta$, $-\zeta/2$, $\zeta/2$, and $\zeta/2$, respectively.[18] The ground-state term of the high-spin $t_{2g}^3e_g$ configuration, ^5E_g, is not split by the spin-orbit interaction. It may be decomposed as $A_1 + T_1 + A_2 + E + T_2$ in the double-group scheme. The matrix elements of H_{so} between the terms of high- and low-spin configurations are $-\sqrt{2\zeta}$, $\sqrt{3/2\zeta}$, $-\zeta$, and $-1/\sqrt{2\zeta}$ for the sublevels A_1, T_1, E_2, and T_2, respectively. However, the ground state of the high-spin $t_{2g}^3e_g$ state is expected to undergo large distortions due to the Jahn-Teller effect. As a result the state splits into two and one cannot use the simple symmetry classifications. The exact value of the electronic coupling is not known but it has to be of the order of ζ as above. The free ion values of ζ are 230 cm^{-1} for Cr(II) and 355 cm^{-1} for Mn(III).[22]

d^7 Ions (Co(II)). A similar situation exists with the d^7 complexes. The high-spin $(t_{2g}^5e_g^2)$ $^4T_{1g}$ state is split by the spin-orbit interaction.[18] The low-spin $(t_{2g}^6e_g)$ ^2E_g ground state is not split by the spin-orbit coupling but a large Jahn-Teller distortion is expected. Therefore, it is difficult to do more than estimate the electronic coupling to be of the order of magnitude of ζ. The free ion value of ζ for Co(II) is 515 cm^{-1},[22] so we take $|V| \simeq 500$ cm^{-1} for this ion.

An interesting conclusion emerging from this calculation of the spin-orbit coupling terms is that the first-order contributions (wherever these are nonvanishing) are comparable in their magnitude to second-order contributions (which appear for the cases when the first-order term vanishes). This conclusion is somewhat surprising as one might have argued, on the basis of simple perturbation-type arguments, that second-order terms should be smaller than first-order contributions. We have searched for contributions of higher order terms to V and found these to be negligible.

IV. Rate Constants. Comparison with Experiments

We shall now attempt to rationalize the available experimental data in terms of our theory. For octahedral complexes the rate constant $k(|V|^2,p,S,\omega,T)$ is given by eq 3 and 8, where only the totally symmetric vibrational mode A_{1g} with its coupling parameter S and frequency ω appears. Unfortunately, all the systems for which the rate constants were measured deviate from strict octahedral symmetry. Consequently, one has to take into account configurational changes in several vibrational modes. In the evaluation of S one has to sum up all the modes, which are characterized by displacements $\Delta r_\kappa \neq 0$, so that the coupling parameter S is

$$S = \sum_\kappa m_\kappa\omega_\kappa(\Delta r_\kappa)^2/2\hbar \tag{14}$$

However, we may still assume that the dominant contribution to S originates from the metal-ligand bonds. Since a detailed normal mode analysis is not practical for the complexes for which spin conversion rates were measured, we use a model of local vibrational modes. The numerical value of S is estimated by using characteristic frequencies for the metal-ligand bonds taken from analogous compounds. The mass associated with these modes is approximated as the mass of the atom which is directly bound to the metal. The change in bond length between the low- and high-spin states of a given complex is not directly measurable. The available information is the bond lengths in several similar complexes, from which one obtains an averaged value for Δr. As a result there is some uncertainty regarding the value of Δr in any specific case.

Finally, we have to consider how to obtain the proper value of the reduced energy gap given by the parameter p in eq 6 and 8. As was already mentioned in section II, the present theory does not consider fully the reaction entropy and, therefore, there is some ambiguity regarding the proper value of the parameter p. As $\Delta G^\circ \sim 0$ we use, as was already discussed, the value $p = 0$ for the calculation of G in Figure 4. One has to remember that this choice of the energy gap introduces further uncertainties in the final numerical result for the rate constant.

Our procedure to estimate the rate constants is to obtain the value of S, eq 14, using the spectroscopic data for the metal-ligand frequency $\hbar\omega$ and structural data for the change in the metal-ligand bond lengths Δr_κ accompanying spin crossover. We then utilize these values of S and of $x = \hbar\omega/k_BT$, together with the data of Figure 4, to obtain the value of $\hbar\omega/g_f|V|^2k$. Finally, the low-spin and high-spin rate constant k is obtained by utilizing the results of section III for the electronic coupling term V and the final-state electronic degeneracy g_f. These theoretical values of k are confronted with the available experimental results. Data on the rates of spin conversion in solutions have only recently become available. Relaxation times down to about 30 ns have been measured using the techniques of the Raman laser temperature jump.[7] More recently, the time domain was extended by the ultrasonic absorption technique and relaxation times down to about 2 ns were measured.[8,12]

For iron(III) complexes spin conversion rate constants of about 5×10^7 and 2×10^8 s^{-1} were found for spin conversion in $[Fe(Sal_2trien)]^+$ and in $[Fe(acac_2trien)]^+$,[12] respectively. For $[Fe(benzac_2trien)]^+$ an upper limit of 1 ns was obtained for the relaxation time (i.e., $k_1, k_{-1} \geq 5 \times 10^8$ s^{-1}).[12] In the case of $[Fe(Et_2dtc)_3]$ no excess sound absorption could be observed,[8] which indicates a rate constant greater than 10^9 s^{-1}. Recent measurements by the Raman laser temperature-jump technique on complexes with substituted Salmeen ($[Fe(X\text{-}Salmeen)_2]^+$) yield rate constants in the range 10^7–10^8 s^{-1}.[11] Most of the measured complexes are of the form $Fe^{III}N_4O_2$. Our estimate of the spin conversion rate constant is based on using a vibrational frequency of 500 cm^{-1} for both Fe(III)-N and Fe(III)-O bonds[24] and changes in bond length upon spin conversion of 0.17 and 0.04 Å for these bonds, respectively.[25] Inserting these values in eq 14 gives $S = 13$, and on looking at Figure 4 ($\hbar\omega/k_BT \sim 2.5$) one obtains $(\hbar\omega/|V|^2g)k \sim 10^8$ cm s^{-1}. In the case of Fe(III) $g_f = 6$ for both high-spin and low-spin states, $\hbar\omega = 500$ cm^{-1}, and $|V| = 44$ cm^{-1}, which gives $\hbar\omega/|V|^2g_f \sim 0.04$ cm. So we finally obtain for the rate constant the value $k \simeq 2 \times 10^9$ s^{-1}. A similar procedure for the case of tris(thiocarbamato)iron(III), based on an average metal-ligand frequency of 340 cm^{-1}[26] and a change in Fe-S

bond length of 0.11 Å,[27] gives $S = 12$, $\hbar\omega/k_BT \sim 1.7$, and the estimated rate constant is $k \simeq 3 \times 10^{10}$ s^{-1}.

The measured spin conversion rates for iron(II) complexes are somewhat smaller than the rates found in iron(III) complexes. At 25 °C the values $k_1 = 5 \times 10^6$ s^{-1} and $k_{-1} = 2.5 \times 10^7$ s^{-1} were measured for Fe(HB(pz)$_3$)$_2$ in THF,[8] and $k_1 = 1.7 \times 10^7$ s^{-1} and $k_{-1} = 7.2 \times 10^6$ s^{-1} for Fe(papth)$_2^{2+}$ in water.[8] Some other measurements by the Raman laser temperature-jump technique gave similar values for the rate constants.[4,5,7] In order to obtain theoretical estimates for the value of the rate constant one needs numerical values for the parameters Δr, ω, and m. There is a large uncertainty in their values. If we take for Δr the value 0.26 Å (obtained as the difference in bond lengths between high-spin [Fe(6-Mepy)$_3$tren]$^{2+}$ (μ_B = 5.0) and low-spin [Fe(py)$_3$tren]$^{2+}$ (μ_B = 0.05),[28,29] $\hbar\omega = 300$ cm^{-1},[24] $m = 14$, we obtain $S = 26$. For this value, using Figure 4, we have $(\hbar\omega/|V|^2 g_f)k \sim 5 \times 10^6$ cm s^{-1}. Taking $V = 170$ cm^{-1}, according to the results of the previous section, we obtain $k/g_f = 5 \times 10^8$ s^{-1}. At this point, we have to comment on the values of the degeneracy factors for the high-spin and the low-spin states of Fe(II). In octahedral symmetry the high-spin state is $^5T_{2g}$ with $g = 15$. However, spin-conversion rates were measured for complexes which deviate from octahedral symmetry. Thus, the spatial degeneracy is expected to be removed and we expect $g = 5$ due only to the contributions of the electronic spin. For the low-spin Fe(II), with the $^1A_{1g}$ state in octahedral symmetry, the degeneracy factor $g = 1$ will remain in lower symmetries as well. Thus, we can provide a very crude estimate of $k \sim 1 \times 10^9$ s^{-1} for this system, which is somewhat higher than the experimental values. Some comments about the uncertainties involved in the calculation of the nuclear term for spin conversion in Fe(II) are in order. The value we have used for Δr is the largest known difference in bond lengths. As the measurements are performed on complexes with different ligands, and not always in pure spin states, it is very difficult to assign a characteristic value for Δr. Churchill et al.[30] and Dose et al.[7] estimate that Δr is in the range of 0.15–0.17 Å. A computation based on this estimate (other parameters being taken as before) gives smaller values for S and therefore higher values for the rate constant.

There are also some measurements of the spin conversion rates in Co(II) complexes. Rates of the order 5×10^6 s^{-1} were observed for [Co(N-R-2,6pyAld)$_2$]$^{2+}$,[13] and rates larger than 10^9 s^{-1} are estimated for [Co(terpy)$_2$]$^{2+}$.[8] There is no experimental information about Δr in such systems and, as was discussed in the previous section, there are difficulties in the quantitative estimate of the electronic coupling. Therefore, we do not attempt to provide a theoretical value for the rate constant.

V. Concluding Remarks

We have described the spin crossover process in terms of a nonadiabatic multiphonon radiationless transition between two (zero order) nuclear potential surfaces corresponding to two different electronic configurations, i.e., different spin states. We shall now consider the approximations inherent in this quantum-mechanical description, which pertain to some general problems as well as to technical details.

From the point of view of general methodology, we have to consider the applicability of the nonadiabatic formalism, which stems from a first-order description of the time evolution of the system. The adequacy of the nonadiabatic description implies that the electronic coupling, V, or the electronic coupling dressed by vibrational overlap terms, should be small relative to some characteristic energies accompanying the nuclear motion, which is specified by the parameters $\hbar\omega$ and S for the internal motion of the complex and by the parameters $\hbar\omega_S$ (solvent characteristic frequency) and E_S for the solvent. Two criteria for the applicability of the nonadiabatic limit may be considered. Firstly, we may disregard altogether the modulation by the solvent and focus attention on the quasi-one-dimensional motion along the coordinate(s) of the complex. The Landau–Zener nonadiabatic limit[15] is attained provided that $Y = |V|^2/\hbar\omega\sqrt{S\hbar\omega k_BT} < 1$, so that for characteristic values of $V = 100$ cm^{-1}, $\hbar\omega = 500$ cm^{-1}, and $S = 15$ we get $Y = 0.1$, and this validity condition is satisfied. Next, we may consider the internal motion modulated by the solvent. In this case we suppose that the vibronic term $|V|^2 G^{(FC)}$, which corresponds to the electronic term modified by a vibrational Franck–Condon factor $G^{(FC)}$, would be small relative to solvent modulation efficiency, so that $\xi = |V|^2 G^{FC}/\hbar\omega_S\sqrt{E_S k_B T} < 1$. For characteristic values of $V \sim 100$ cm^{-1}, $G^{(FC)} \sim \exp(-S) \sim 10^{-6}$, $\hbar\omega_S \sim 10$ cm^{-1}, and $E_S \sim 100$ cm^{-1}, we estimate $\xi = 10^{-3}$ and this validity condition is well obeyed. These rough estimates inspire some confidence in the applicability of the nonadiabatic limit.

Next, we consider the hidden approximations involved in the general nonadiabatic rate equation. Equations 2 and 5 are quite general, involving only the Condon approximation, where the spin–orbit coupling term is independent of nuclear coordinates and separating the nuclear motion of the solvent from the inner nuclear motion of the complex. As the vibrational states are not yet specified the partition functions Z_i^s and Z_i^c can be different, in principle, for the low-spin (ls) → high-spin (hs) process as compared to the reverse (hs) → (ls) reaction. Obviously, eq 2 is applicable for both processes. It is important to emphasize that the ratio of the rate constants $k_{ls\to hs}$ and $k_{hs\to ls}$ is in general

$$K \equiv \frac{k_{ls\to hs}}{k_{hs\to ls}} = \frac{g_{hs}}{g_{ls}}\left(\frac{Z^c_{ls}Z^s_{ls}}{Z^c_{hs}Z^s_{hs}}\right)^{-1} \exp(-\Delta E/k_BT) \quad (15)$$

where g_{hs} and g_{ls} are the electronic degeneracies in the (hs) and (ls) states. Equation 15 satisfies the general conditions of detailed balance. The derivation of eq 6 and 8 from the basic eq 2–5 introduced drastic assumptions regarding nuclear motion. First, a small number of harmonic oscillators represents the solvent motion and the internal nuclear motion of the complex. Second, configurational changes are described in terms of the displacements of the minima of the potential surfaces between the initial and the final electronic states, while frequency changes are neglected. This approximation implies that the partition function in the hs and ls states are equal whereupon

$$K = (g_{hs}/g_{ls}) \exp(-\Delta E/k_BT) \quad (16)$$

Third, the effects of configurational changes and entropy effects due to solvent reorganization are disregarded.

In the application of the simplified rate, eq 8, to real systems several technical simplifications were introduced. The calculation of the electronic contribution V is reasonable; however, the numerical computation of the nuclear term G is fraught with difficulties as the spectroscopic and structural input data are unknown. Three parameters are required for specification of G, which are $p = \Delta E/\hbar\omega$, $\hbar\omega$, and S. We have taken $p = 0$ for all our calculations. This is not bad as according to eq 16 we then have $K = g_{hs}/g_{ls}$, which are quite close to the experimental values, i.e., $K \sim 1$. At the present stage of both experiment and theory we feel that the introduction of an additional (small) variable parameter p will be of little value. Spectroscopic values for the relevant frequencies $\hbar\omega$ are scarce. Regarding the calculation of the coupling terms S, which in turn is determined by the displacements Δr_κ, masses m, and frequency ω, we have pointed out already that the structural data for Δr_κ are scarce. Another problem is the value of the effective mass of the vibrational mode. We have used the atomic mass but, as the atom is located in a rigid aromatic ring, it seems reasonable that the effective mass is higher. In such a case, the

computed value of S will become larger and consequently the rate constant smaller. One important factor that we did not incorporate into the calculation of S is the changes in the equilibrium configuration of vibrational modes other than the metal–ligand bonds. From the deviations from octahedral symmetry and the ring structures appearing in all the complexes we have mentioned, it is clear that several other ring modes may contribute to S. It is impossible to give a reasonable quantitative estimate for their effect, but undoubtedly S must be larger than the one appearing in our calculation and, therefore, our estimate of the rate constant given here has to be considered as an upper limit.

From this somewhat lengthy discussion of the technical details of the present calculation it is apparent that the numerical values calculated in section IV for the (ls) $\rightleftarrows$ (hs) rate constants should not be taken too seriously as far as absolute numerical magnitude is concerned. It is, however, quite remarkable that the present quantum-mechanical multiphonon theory led to a reasonable order-of-magnitude estimate of the rate constants for this class of processes without the use of any adjustable parameters. In particular, the present theory has been useful in the elucidation of electronic and nuclear contributions to the rate constants for this class of processes. We feel that rate process in condensed phases, such as (ls) $\rightleftarrows$ (hs) crossover considered herein, should be described in terms of multiphonon theories of radiationless transitions, which are more reliable and informative than the conventional absolute reaction rate theory.

References and Notes

(1) Cambi, L.; Cagnoro, A. *Atti Accad. Naz. Lincei* **1931,** *13,* 809.
(2) Martin, R. L.; White, A. H. *Transition Met. Chem.* **1968,** *4,* 113.
(3) Barefield, E. K.; Busch, D. B.; Nelson, S. M. *Q. Rev., Chem. Soc.* **1968,** *22,* 457.
(4) Beattie, J. K.; Sutin, N.; Turner, D. H.; Flynn, G. W. *J. Am. Chem. Soc.* **1973,** *95,* 2052.
(5) Hoselton, M. A.; Drago, R. S.; Wilson, L. J.; Sutin, N. *J. Am. Chem. Soc.* **1976,** *98,* 6967.
(6) Reeder, K. A.; Dose, E. V.; Wilson, L. J. *Inorg. Chem.* **1978,** *17,* 1071.
(7) Dose, E. V.; Hoselton, M. A.; Sutin, N.; Tweedle, M. F.; Wilson, L. J. *J. Am. Chem. Soc.* **1978,** *100,* 1141.
(8) Beattie, J. K.; Binstead, R. A.; West, R. J. *J. Am. Chem. Soc.* **1978,** *100,* 3044.
(9) Dose, E. V.; Murphy, K. M. M.; Wilson, L. J. *Inorg. Chem.* **1976,** *15,* 2622.
(10) Tweedle, M. F.; Wilson, L. J. *J. Am. Chem. Soc.* **1976,** *98,* 4824.
(11) Petty, R. H.; Dose, E. V.; Tweedle, M. F.; Wilson, L. J. *Inorg. Chem.* **1978,** *17,* 1064.
(12) Binstead, R. A.; Beattie, J. K.; Dose, E. V.; Tweedle, M. F.; Wilson, L. J. *J. Am. Chem. Soc.* **1978,** *100,* 5609.
(13) Simmons, M. G.; Wilson, L. J. *Inorg. Chem.* **1977,** *16,* 126.
(14) (a) Austin, K. H.; Beeson, K. W.; Eisenstein, L.; Frauenfelder, H.; Gunsalus, I. C. *Biochemistry* **1975,** *14,* 5355. (b) Jortner, J.; Ulstrup, J. *J. Am. Chem. Soc.* **1979,** *101,* 3744.
(15) Levich, V. G. In "Physical Chemistry: An Advanced Treatise", Eyring, H., Henderson, D., Jost, W., Eds.; Academic Press: New York, 1970; Vol. 9B.
(16) Kestner, N. R.; Logan, J.; Jortner, J. *J. Phys. Chem.* **1974,** *78,* 2148.
(17) Buhks, E.; Bixon, M.; Jortner, J.; Navon, G. *Inorg. Chem.,* **1979,** *18,* 2014.
(18) Griffiths, J. S. "Theory of Transition Metal Ions"; Cambridge University Press: New York, 1961.
(19) Tanabe, Y.; Sugano, S. *J. Phys. Soc. Jpn.* **1954,** *9,* 766.
(20) (a) Jørgensen, C. K. "Absorption Spectra and Chemical Bonding in Complexes"; Pergamon Press: Oxford, 1962. (b) *Prog. Inorg. Chem.* **1962,** *4,* 73.
(21) Gerloch, M.; Slade, R. C. "Ligand Field Parameters"; Cambridge University Press: New York, 1973; p 214.
(22) Dunn, T. M. *Trans. Faraday Soc.* **1961,** *57,* 1441.
(23) Figgis, B. N. "Introduction to Ligand Fields"; Interscience: New York, 1966.
(24) Ferraro, J. R. "Low Frequency Vibrations of Inorganic and Coordination Compounds"; Plenum Press: New York, 1971.
(25) Sinn, E.; Sinn, G.; Dose, E. V.; Tweedle, M. F.; Wilson, L. J. *J. Am. Chem. Soc.* **1978,** *100,* 3375.
(26) Hall, G. R.; Hendrickson, D. N. *Inorg. Chem.* **1976,** *15,* 607.
(27) Leipoldt, J. G.; Coppens, P. *Inorg. Chem.* **1973,** *12,* 2269.
(28) Mealli, C.; Lingafelter, E. C. *Chem. Commun.* **1970,** 885.
(29) Hoselton, M. A.; Wilson, L. J.; Drago, R. S. *J. Am. Chem. Soc.* **1975,** *97,* 1722.
(30) Churchill, M. R.; Gold, K.; Maw, Jr., C. E. *Inorg. Chem.* **1970,** *9,* 1597.

Chiral Discrimination in Excimer Formation

Chieu D. Tran and Janos H. Fendler*

Contribution from the Department of Chemistry, Texas A&M University, College Station, Texas 77843.

Received November 20, 1978

Abstract: Steady-state and nanosecond time resolved spectroscopy have been used to determine parameters for excimer formation for *N*-[4-(1-pyrene)butanoyl]-D-tryptophan methyl ester (pyr-D-Trp), *N*-[4-(1-pyrene)butanoyl]-L-tryptophan methyl ester (pyr-L-Trp), and their racemate, pyr-DL-Trp, in methanol and for pyr-D-Trp in optically active (*R*)-(−)-2-octanol, (*S*)-(+)-2-octanol, and racemic (*RS*)-(±)-2-octanol. Appreciable differences have been noted between the behavior of the pure enantiomer and its racemate in MeOH. Thus, the rate constant of excimer formation for pyr-DL-Trp, $(6.9 \pm 0.5)\ 10^9\ M^{-1}\ s^{-1}$, is greater than those for the pure enantiomers, $(4.0 \pm 0.7)\ 10^9\ M^{-1}\ s^{-1}$. The quantum efficiency of pyr-DL-Trp excimer formation ($q_D/q_M = 0.7 \pm 0.1$) is smaller than that for pyr-D-Trp or pyr-L-Trp ($q_D/q_M = 1.1 \pm 0.2$). Differences in equilibrium constants for excimer formation indicated a chiral discrimination energy of 700 cal mol^{-1}. Chiral discrimination originates in differential electrostatic, dispersion, and resonance interactions. Appreciable differences have also been observed in the kinetic and thermodynamic parameters for pyr-D-Trp excimer formation in (*R*)-(−)-2-octanol and (*S*)-(+)-2-octanol.

Introduction

Differences in crystal structures, melting points, boiling points, solubilities, and ^1H NMR spectra between a pure enantiomer and its racemate have been recognized for some time.[1-10] Similarly, there are examples of enantiomeric excess dependent reaction rates and product distributions.[6,7] Enantiomeric effects[11] are the results of interactions between two chiral molecules which discriminate between like (*d* with *d* or *l* with *l*) and unlike (*d* with *l* or *l* with *d*) pairs. They have been treated theoretically in terms of short- and long-range nonbonded interactions.[8,10]

Dynamic investigations of photochemical processes[12] can provide a wealth of information on factors which determine enantiomeric discriminations. We have initiated, therefore, systematic studies on excimer formation[13] involving chiral molecules. *N*-[4-(1-Pyrene)butanoyl]-D-tryptophan methyl ester (pyr-D-Trp) and *N*[4-(1-pyrene)butanoyl]-L-tryptophan methyl ester (pyr-L-Trp) have been utilized in the present work. Using steady-state and nanosecond time resolved fluo-

0002-7863/80/1502-2923$01.00/0